

Structure and Properties of Isotactic Polypropylene Functionalized by Ultraviolet Irradiation

RONG GUAN, XI XU

Polymer Research Institute of Chengdu University of Science & Technology, Chengdu, 610065, People's Republic of China

Received 22 November 1999; accepted 12 May 2000

ABSTRACT: The structural, crystalline, thermal, morphological, and mechanical properties of isotactic polypropylene (iPP) functionalized by lower energy ultraviolet (UV) irradiation are studied by means of infrared spectroscopy (IR), differential scanning calorimetry (DSC), wide-angle X-ray diffraction (WAXD), thermogravimetry (TG), thermomechanical analysis (TMA), polariscope, and mechanical measurements. After the UV irradiation in less than a few hours, the oxygen containing polar groups have been introduced onto iPP chains. DSC analysis shows that a new melting peak is observed around 150°C for the UV irradiated iPP, indicating that there is a α -phase to β -phase transition during UV irradiation process. Under polariscope, the morphology of the UV irradiated iPP is changed, and the deformed α -phase morphology can be observed. DSC and WAXD analysis reveal for the crystallinity of the UV-irradiated iPP increase with UV time, but the relative level and the order of β -phase increase and then decrease with increasing UV time. Under the controlled UV time, the thermomechanical deformation of iPP decrease, and the initial and final thermal degradation temperature of iPP rises up by 70 to 125°C higher, respectively, indicating that the UV-irradiated iPP has higher thermal stability than the non-UV irradiated iPP. The tensile and impact strength, the elongation at break, and the Young's modulus of the UV-irradiated iPP are enhanced, exhibiting the toughened and strengthened effects. © 2000 John Wiley & Sons, Inc. *J Appl Polym Sci* 79: 1456–1466, 2001

Key words: polypropylene; ultraviolet; irradiation; structure; property

INTRODUCTION

Functionalization polypropylene (PP) is one of the ways to enhance the compatibility of the nonpolar polypropylene with other engineering plastics or inorganic fillers.¹ Functionalizing polypropylene through the irradiation techniques has the advantage of having no chemical pollution and no residual monomer that might bring some nega-

tive effects on the material if it stays in the polypropylene. Since the 1990s, Xu Xi² has made a creative breakthrough. Xu et al. have used γ -ray, electron beam, ultraviolet, and microwave irradiation techniques to functionalize polyethylene (PE) without adding any monomers and auxiliaries in air, significantly enhancing the compatibility of PE with other engineering plastics and the inorganic fillers, and have obtained strengthened and toughed PE blends.

Polypropylene, when subjected to irradiation of γ -ray, electron beam, and ultraviolet in air, primarily undergoes chain scission^{3–7}; the higher the

Correspondence to: R. Guan.

Journal of Applied Polymer Science, Vol. 79, 1456–1466 (2001)
© 2000 John Wiley & Sons, Inc.

irradiation energy, the more chain scission of polypropylene. Although the response of polymers to various radiation sources depends on such parameters as the polymer structure, the radiation wavelength, intensity and duration, temperature, and environment,⁸ the lower energy irradiation is more suitable for polypropylene.

Of polypropylene, upon ultraviolet irradiation over several hundred hours, its properties will be decreased due to polypropylene's photo-oxidation degradation.⁹ There has been a lot of research dealing with the kinetics and the degradation products of polypropylene.^{10–15} For polypropylene photo-oxidation under natural and accelerated oxidation conditions, hydroperoxides were the primary photoproducts, and ketones were the dominant oxidation products.¹⁶ There is no doubt that the photo-oxidation degradation under long-time ultraviolet irradiation conditions causes the deterioration of polypropylene mechanical characteristics, but the short time and lower energy ultraviolet irradiation can be very useful in modifying polypropylene properties. Shukla,¹⁷ Nito,¹⁸ and Zhang¹⁹ et al. used lower energy ultraviolet irradiation to graft 2-hydroxyethyl methacrylate, acrylonitrile, acrylic acid, and acrylamide onto polypropylene. Pasternak²⁰ combined the photo-oxidation and photosubstitution to modify the polypropylene surface property, whereas Uzo-mak et al.,²¹ studying the outdoor weathering of polypropylene films, found that the ultimate mechanical properties of polypropylene films increased a small amount in less than 240 exposure hours. Therefore, it is possible to use lower energy ultraviolet irradiation to modify polypropylene properties.

Until now, very few works have deal with polypropylene functionalization through irradiation techniques to be used in polypropylene blends. This study deals with the structural, crystalline, thermal, morphological, and mechanical properties of isotactic polypropylene, which is ultraviolet irradiated in less than 2.5 h to introduce the polar groups onto isotactic polypropylene chains through the physical ways so as to prevent chemical pollution. Infrared spectroscopy is used to characterize the polar groups after ultraviolet irradiation of isotactic polypropylene. Differential scanning calorimetry (DSC) and wide-angle X-ray diffraction measurements (WAXD) are used for the determination of the crystallinity as a function of ultraviolet irradiation time. The thermal degradation temperature and the thermome-

chanical deformation are determined by thermogravimetry (TG) and thermomechanical analysis (TMA), respectively. Polariscope is employed for investigation of effect of UV irradiation time on the isotactic polypropylene morphology. The mechanical measurements are carried out to study the mechanical properties of isotactic polypropylene before and after UV irradiation.

EXPERIMENTAL

Materials

A commercial grade of iPP (PP2401, Yanshan Petrochemistry Company of China) was used, with an M_w value of 240,000, the melt index 2.5 g/10 min and the density ranged from 900 to 910 kg/m³.

Ultraviolet Irradiation

A 500-W Ga-I lamp manufactured by Chengdu Lamp Factory of China was used. The Ga-I lamp is in a tube shape, with a wavelength in the range of 340–370 nm, the ultraviolet intensity 3.2×10^{-2} W/m², and is initiated by a point contactor. The UV irradiation was operated at room temperature in air. The iPP specimens were placed under the lamp in a set distance 28 cm.

Specimen Preparation

The iPP films used to study the crystalline and thermal properties by DSC, WAXD, TG, and TMA were prepared by melting the iPP pellets at $192 \pm 2^\circ\text{C}$, pressing in a hot and cold hydraulic press successively. The thickness of iPP polypropylene film is about 30–40 μm . To prepare bar specimens, the UV irradiated iPP pellets were mixed in a two-roll mill at $168 \pm 2^\circ\text{C}$ for 12 min. The milled iPP was then melted and pressed at $192 \pm 2^\circ\text{C}$, 4 MPa for a few minutes by a hot hydraulic press, then cooled down under 8 MPa pressure at room temperature for 15 min by a cold hydraulic press to produce iPP plates. These iPP plates were cut into the bar specimens according to the testing standards by an all-purpose machine. The films for polariscope analysis were prepared by melting the polymer in the press at 192°C , then isothermally crystallizing at 130°C for 1 h.

FTIR Infrared Spectroscopy

FTIR analysis was performed using a Nicolet 560 series FT-infrared spectrometer. The films were

scanned from 4000 to 400 cm^{-1} with a resolution of 4 cm^{-1} , scanning number 26.

Differential Scanning Calorimetry (DSC)

Calorimetric measurements were carried out on a Dupont 2910 thermal analysis system with the software V4.10. The sample weighing was carried out on a DuPont TG2950 with specimens 3–4 mg each, and the thermograms were recorded under nitrogen flow ($1 \times 10^{-5} \text{ m}^3/\text{min}$) using a heating rate of $10^\circ\text{C}/\text{min}$, from room temperature to 190°C . To erase any thermal history, a reheating scan (the second heating run) was conducted with the same heating rate after the specimen were heated to 190°C and cooled down in air. The melting temperature (T_m) and heat of fusion or enthalpy (ΔH_m) were measured from thermograms. Degree of crystallinity was also determined from $\chi = \Delta H_m / \Delta H_m^\circ \%$ (where for PP, the equilibrium heat of melting $\Delta H_m^\circ = 209 \text{ J/g}$).

Wide-Angle X-ray Diffraction (WAXD)

WAXD analysis was performed using a MaxIII A (Rigaku) wide-angle X-ray diffractometer (Ni-filtered $\text{CuK}\alpha$ radiation). The high voltage was 35 kV, tube current 20 mA, and the wavelength 1.54 nm in the diffraction angle range $2\theta = 10\text{--}49^\circ$.

Thermogravimetry (TG)

TG measurements were carried out on a DuPont 2950 thermal analysis system in a heating rate $10^\circ\text{C}/\text{min}$, nitrogen flow $1 \times 10^{-5} \text{ m}^3/\text{min}$. Temperature was set from room temperature to 400°C , or over 400°C if the specimen does not degrade completely.

Thermomechanical Analysis (TMA)

TMA analysis was performed using a Dupont 2000 thermomechanical analyzer, at a heating rate $10^\circ\text{C}/\text{min}$ from room temperature to 160°C . The specimen has the dimension: length 4 mm, width 4 mm, and thickness 4 mm.

Polariscope Observation

Polariscope observations were carried out on the isothermally crystallized iPP samples at room temperature, using a LEITZ polariscope using a $400\times$ amplify camera lens.

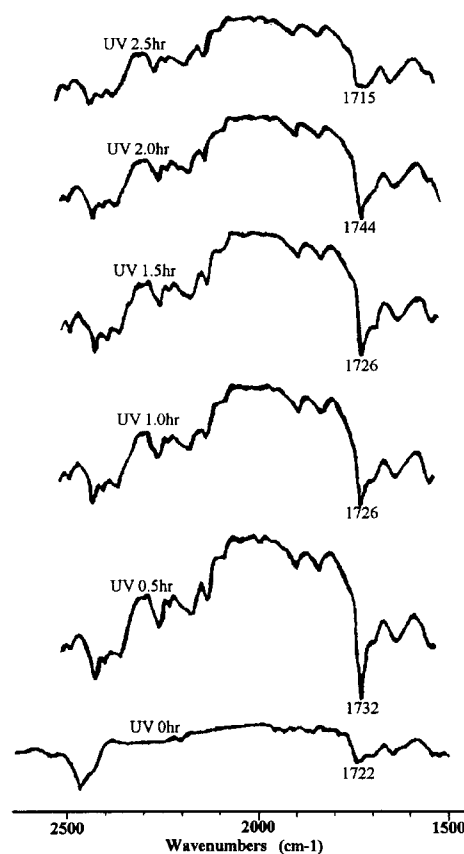


Figure 1 FTIR spectra of iPP before and after UV irradiation.

Mechanical Measurement

Tensile and flexural measurements were carried out on an Instron 4302 all-purpose tester. The specimens were cut into dumbbell shapes, the size of specimens and test conditions were followed the ASTM D268. The flexural measurements were operated at the speed of 2 mm/min, and the set depth 6 mm in a three point bending way. The specimen size for flexural measurement was 80 mm long, 10 mm wide, and 4 mm thick. The impact strength measurements were operated according to ISO180-1993E standard. The results reported here are the average of five tests.

RESULTS AND DISCUSSION

FTIR Infrared Spectroscopy

Figure 1 is the FTIR spectra of iPP before and after UV irradiation. It is apparent that the absorption bands around the 1720 cm^{-1} for the UV

Table I IR Absorption Maximal of Some Model Carbonyl Compounds

Compound	Carbonyl Type	λ_{\max} cm^{-1}
Methyl <i>n</i> -butyrate Ethyl acetate	$\begin{array}{c} \text{O} \\ \\ -\text{C}-\text{C}-\text{O}-\text{C}- \\ \quad \quad \end{array}$	1746 (1748–1738)
2-Methyl-4-pentanone 2-Undecanone	$\begin{array}{c} \text{CH}_3 \\ \\ -\text{CH}_2\text{C} \\ \\ \text{O} \end{array}$	1726 (1725)
2'6-Dimethyl-4-heptanone 2'6'8-Trimethyl-4-nonanone	$\begin{array}{c} \text{CH}_3 \quad \text{O} \quad \text{CH}_3 \\ \quad \quad \\ -\text{C}-\text{C}-\text{CH}_2-\text{C}-\text{CH}_2-\text{C}- \\ \quad \quad \quad \\ \text{H} \quad \quad \quad \text{H} \end{array}$	1717 (1721)

irradiated iPP increase, indicating that the UV irradiation does introduce the polar groups onto iPP chains. Because two stretching vibration bands at $1820\text{--}1810\text{ cm}^{-1}$ and $1800\text{--}1780\text{ cm}^{-1}$ do not appear, the UV irradiation does not bring the peroxy acid groups onto iPP chains.⁷ Comparing the absorption bands in Figure 1, and Tables I²² and II,²³ it can be said that the $-\text{C}(=\text{O})\text{OC}-$, $-\text{C}(=\text{O})\text{CH}$ and $-\text{CH}_2\text{C}(=\text{O})\text{CH}_2-$, etc., oxygen-containing polar groups have been introduced onto iPP chains through UV irradiation.

Differential Scanning Calorimetry

To erase any thermal history, a second thermal scan was conducted. Figure 2 shows DSC traces of the UV irradiated iPP (UV iPP) at 0, 0.5, 2.0, and 2.5 h. It is apparent that there are two melting peaks on the second heating thermograms for the iPP UV irradiated 0.5 and 2.0 h, and the same to the iPP UV irradiated 1.0 and 1.5 h (their DSC

thermograms are not shown here). This means that there are at least two kinds of crystallinities in the UV irradiated iPP. The two melting peaks on the DSC curve for the UV iPP are around 150 and 165°C , which represent melting of the β -phase and α -phase,²⁴ respectively, indicating that there is an α -phase to β -phase transition during the UV irradiation process. Figure 3 shows a comparison of DSC thermograms between the non-UV irradiated iPP and the UV irradiated iPP. It can be seen that the small melting peak of the β -phase increases with UV time. Its relative level will be discussed in WAXD analysis later on.

From Figure 2 it can be seen that there is only one melting peak even in the second melting thermogram for the iPP UV irradiated 2.5 h. One of the reasons for this is that at such a relatively long UV irradiation time, there is more chain scission occurring, and these degraded chains are easier to pack into crystal lattices to form a stable α -phase. Another reason is owing to the reorganization of a phase with relatively low stability during subsequent heating in DSC.²⁵ When iPP is irradiated under UV, the oxygen-containing group will be introduced onto iPP chains and at the same time some chains of iPPP will degrade. The degraded iPP chains are easier to reorganize to the phase. When the UV irradiated iPP is subjected to heat to melt, the chains containing the oxygen group will degrade too and thus increase the amount of the degraded chains, which will pack into crystal lattices to form a stable α -phase.

Table II FTIR Values for Identification and Qualification of Ketone Groups in Polyolefin Oxidation Products

Carbonyl Group	Absorption (cm^{-1})
$\text{R}-\text{C}(=\text{O})-\text{CH}_3$	1724
$\text{R}-\text{C}(=\text{O})-\text{CH}_2^{\sim}$	1718
$\text{R}-\text{C}(=\text{O})-\text{OCH}_2^{\sim}$	{ 1744 1190

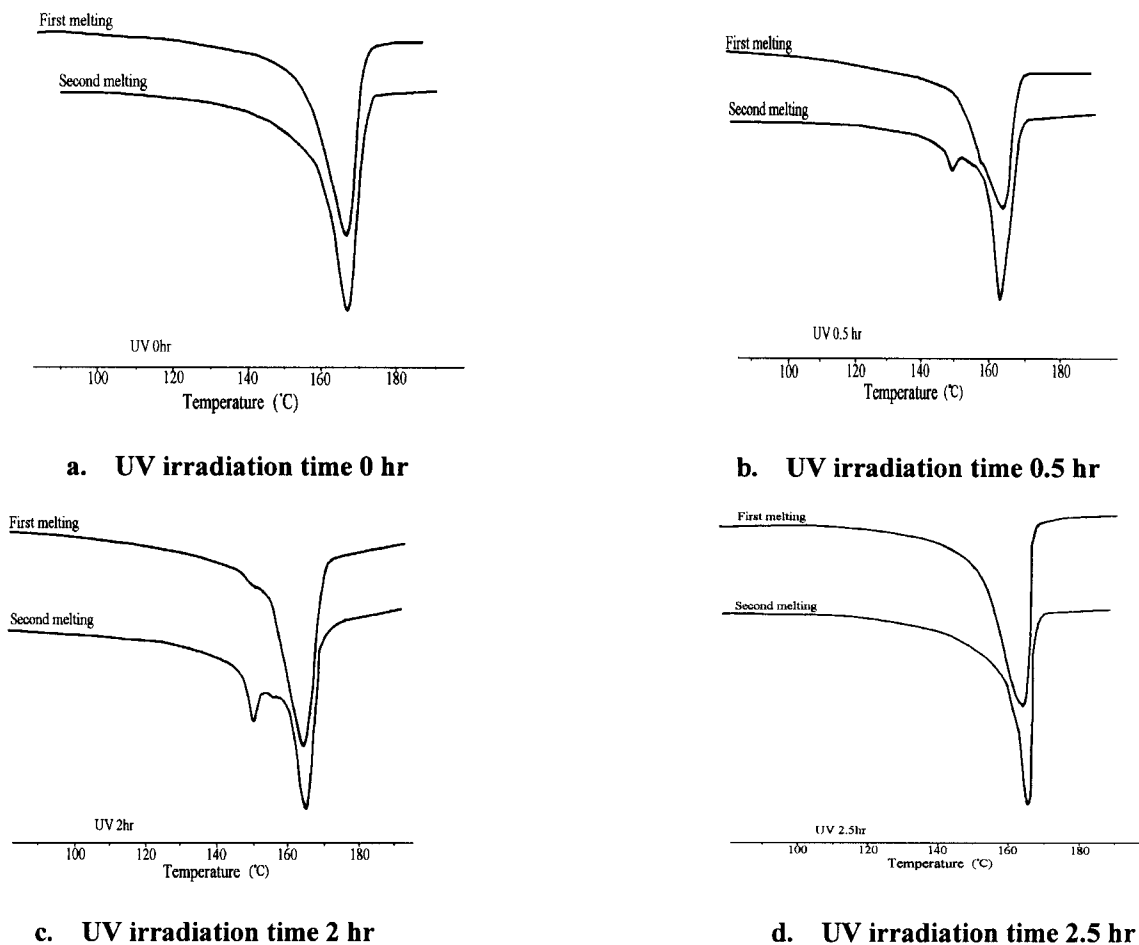


Figure 2 The first and second melting thermograms of the UV irradiated iPP.

The DSC data for investigating the crystallization and melting behavior of the UV iPP are presented in Table III and Table IV. It can be seen that under the experimental conditions examined, the melting peak temperature (T_p) for the UV iPP drops 1 to 3°C due to the crystal lattice defects and changes in crystal volume caused by the UV irradiation. From Table III and Table IV, we can also see that within 2.0 h all the UV iPP display two melting peaks around 150 and 165°C, proving the appearance of the β -phase. The usual way to obtain β -phase iPP includes adding some additives such as β nucleating agents, and control the cooling rate, crystallization temperature, and melting temperature.²⁶ But here we obtain β -phase iPP only through short-time UV irradiation. This should be a very useful way to obtain β -phase iPP, as β -phase iPP has a higher tensile and impact strength than the α -phase iPP.²⁷

For the melting enthalpies of the UV iPP listed in Table III and Table IV, the general trends are

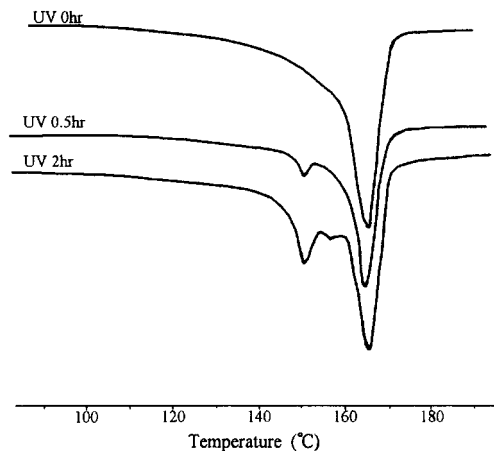


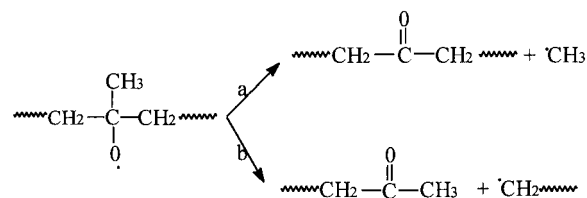
Figure 3 Comparison of the second thermograms of the UV irradiated iPP.

Table III The First Melting DSC Data of UV-Irradiated iPP

UV Time (h)	T_p (°C)	T_{onset} (°C)	Enthalpy (J/g)	Crystallinity (%)
0	168	156	72.7	34.8
0.5	166	153	53.7	25.7
1.0	165	156	69.7	33.3
1.5	166	153	83.7	40.1
2.0	167	155	84.5	40.4
2.5	165	156	135.4	64.8

similar for the two runs of the samples. For the first melting enthalpy in Table III, there is a decrease for the UV 0.5 h specimen, and afterward, the enthalpy increases with UV time. For the second heating run, the variation of enthalpy with UV time is also similar, with an initial decrease followed by an increase. The effect of UV irradiation time on the degree of crystallinity of iPP is in accord with the variation of the enthalpy. With UV time increases, the degree of crystallinity initial decreases and then increases. When UV time reaches 2.5 h, the degree of crystallinity of iPP increases from 35 to 70%. This should be caused by the fact that the degraded iPP segments are easier to pack into crystal lattice to crystallize, thus increasing the crystallinity of iPP. Comparison the crystallinity in the first heating run with that in the second heating run, the later one is larger than the former. This can be explained as, during the first heating run, some chain segments with the structure defects are adjusted, and the crystal segments with crystal defects in the crystalline area obtain certain energy and pack into crystal lattice to recrystallization.

The crystallinity decrease for the UV 0.5 h sample can be explained as that primary alkyl

**Figure 4** The part scheme of photooxidation of PP.

radicals, created through pathway a and b in Figure 4, will recombine in the cage, leading to crosslinking reaction.¹⁶ Hence, this recombination may also valid for primary alkyl radicals generated in the initial UV irradiation (short-time UV irradiation) to lead to crosslinking. The experimental results of higher energy irradiation show that the crystallinity of polymer will decrease if the polymer shows crosslinking,¹³ or change to an amorphous polymer if the irradiation dose is high enough. The crystallinity variation of the UV 0.5 h iPP is in good agreement with higher energy irradiation observation, so it can be said that the crystallinity reduction for the UV 0.5 h iPP resulted from the crosslinking. However, this kind of crosslinking is an unstable kind of pseudocrosslinking, because when the UV time is larger than 0.5 h, the crystallinity of iPP increases again with increasing the UV time.

Wide-Angle X-ray Diffraction

The d-spacing of several main crystalline plains of the UV iPP are listed in Table V. It is noticeable that the d-spacing of the UV iPP is larger than that of the non-UV iPP. Within 2 h of UV time, the d-spacing of the UV iPP, which can be related to the average size of crystallites, increases with increasing UV time. This means crystallites do break down upon ultraviolet irradiation. And this change can be related to the β -phase appearance and its variation.

Table IV The Second Melting DSC Data of UV-Irradiated iPP

UV Time (h)	T_p (°C)	T_{onset} (°C)	Enthalpy (J/g)	Crystallinity (%)
0	166	159	73.7	35.3
0.5	150 & 163	147 & 159	56.8	27.2
1.0	146 & 163	149 & 157	73.0	34.5
1.5	151 & 165	145 & 157	84.7	40.5
2.0	150 & 165	148 & 159	90.0	43.1
2.5	166	162	145.9	69.8

T_p : peak temperature of melting; T_{onset} : extrapolated initial temperature of melting.

Table V WAXD Analysis of Crystalline Plane of UV Irradiated iPP

UV Time (h)	d-Spacing of UV-Irradiated PP Crystalline Plane (angstrom)			
	(110)	(300)	(130)	(111)
0	6.255	5.466	4.761	4.103
0.5	6.294	5.515	4.792	4.179
1.5	6.396	5.627	4.832	4.182
2.0	6.515	5.617	4.832	4.232
2.5	6.399	5.600	4.830	4.200

The relative levels of the β -phase (hexagonal phase) is usually described in term of the Turner-Jones equation, which is defined as²⁸:

$$K = \frac{H(300)}{H(300) + H(110) + H(040) + H(130)} \quad (1)$$

where H(110), H(040), and H(130) are the height of three strong equatorial α -phase peaks (110), (040), and (130), and H(300) the height of the strong single β -phase peak (300). The order parameter S of the β -phase was calculated by eq (2)²⁶:

$$S = H(300)/[H(300) + H(301)] \quad (2)$$

where H(301) is the height of the peak from the (301) crystalline face of the β -phase. The higher the S value is, the higher the order of the β -phase. From Table VI, it can be seen that with UV time increases from 0.5 h to 2.5 h; the relative level K and the order S of β -phase initially increase and then follow a decrease. Still, the K and S values of the UV 0.5 h iPP are smaller than that of the non-UV iPP due to a pseudocrosslinking. This is in good agreement with DSC analysis in that there is no β -phase melting peak for the UV 2.5 h iPP. However, the degree of crystallinity of the UV PP increases with increasing UV time, being also in accord with the DSC crystallinity variation.

Thermogravimetry

Table VII lists TG analysis results: the initial degradation temperature (T_i), the final degradation temperature (T_f), the middle degradation temperature (T_M), and the corresponding weight loss (W_M), and the peak temperature of DGT

Table VI Crystallinity, K and S Value of the UV-Irradiated iPP

UV Time (h)	Crystallinity (%)	K (%)	S (%)
0	36.7	14.3	39.2
0.5	36.0	12.5	34.4
1.5	43.1	23.6	66.0
2.0	46.1	20.4	50.3
2.5	53.8	11.7	37.9

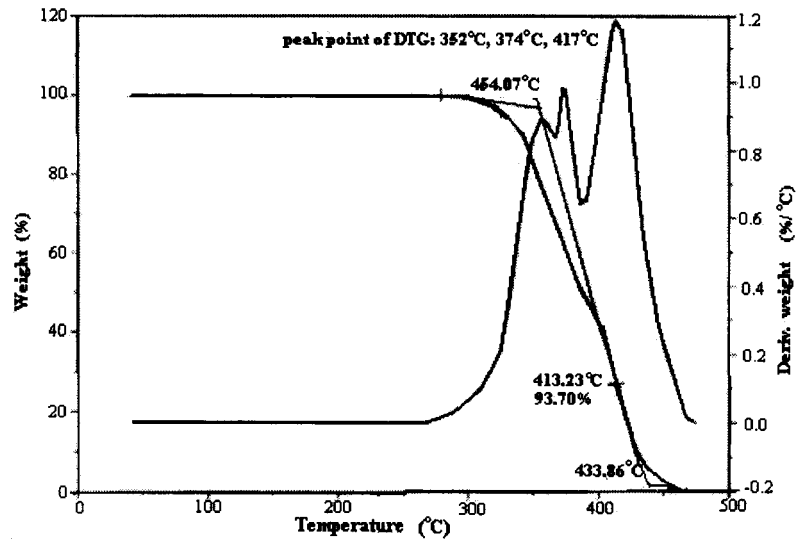
curve (T_p). It is apparent that within 2 h UV time, T_i , T_f , T_M , and T_p of the UV iPP rise up to 79–125°C higher than the non-UV irradiated iPP. Moreover, the UV iPP shows a broad degradation that spans the temperature range from 354 to 434°C; thus, the UV-irradiated iPP have higher thermal stability than the non-UV irradiated iPP.

It is interested to see from Figure 5(b), that the iPP UV irradiated 0.5 h is fairly stable. It starts to degrade at 354°C and against a temperature rise up to 434°C, but the non-UV iPP reveals some weight loss from about 275°C, and lasts only to 309°C. There are three peaks of the maximum degradation rate on DTG curve of the 0.5 h UV iPP, corresponding to temperature 352, 374, and 417°C, but only one at 298°C for the non-UV iPP. This reveals that there are some different structures in the 0.5 h UV iPP, that is, a pseudocrosslinking. Also, when the UV time is larger than 0.5 h, there is only one degradation peak on the DTG curve for the UV iPP, meaning that there is only one degradation mechanism. The improvement in thermal stability for the UV iPP can be explained by increasing crystallinity and introducing the oxygen containing groups onto iPP molecular chains. However, the chain scission during the UV irradiation process will

Table VII TG Analysis of the UV-Irradiated iPP

UV Time (h)	T_i (°C)	T_f (°C)	T_M (°C)	W_M (%)	T_p (°C)
0	275	309	297	95	298
0.5	354	434	413	94	352, 374, 417
1.0	338	397	388	90	386
1.5	341	406	386	89	386
2.0	347	427	388	90	389
2.5	270	310	289	93	288

a. UV time 0 hour



b. UV time 0.5 hour

Figure 5 TG and DTG curves of the UV-irradiated PP.

reduce the thermal stability of iPP. The competition of two factors determines the final thermal stability of iPP. As we can see with the iPP UV-irradiated 2.5 h, its thermal stability is nearly the same as the non-UV iPP due to its relatively large chain scission, so it is better to limited UV time within 2.5 h under the considered experimental conditions.

Thermomechanical Analysis

The thermomechanical deformation traces for the UV iPP studied under nitrogen are shown in Figure 6. At the same temperature, the UV iPP show less deformation than that of the non-UV iPP. On the other hand, the UV iPP have higher thermal size stability than the non-UV iPP. This phenomenon can reduce the thermal swell stress and increase the working lifetime of the UV iPP. Also, the higher thermomechanical deformation stability of the UV iPP is owing to the two effects of increased crystallinity and introduced polar groups.

Polariscope Observation

Figure 7 shows the polariscope micrographs of iPP samples before and after the UV irradiation and isothermally crystallized at 130°C for 1 h. The crystalline morphology of the non-UV iPP is very

clear and perfect [see Fig. 7(a)], showing the exclusive α -phase spherulite, whereas the crystalline morphology of the UV-irradiated iPP [see Fig. 7(b)–(f)] shows an unclear and unperfected spherulite. This suggests that the UV irradiation decreases the effect of iPP crystallizing to the α -phase spherulite but increases its effect to crystallize to the β -phase spherulite combined with the above DSC and WAXD analysis.

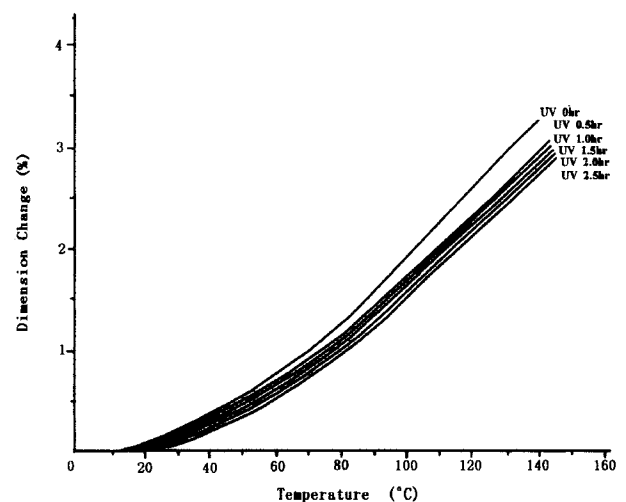
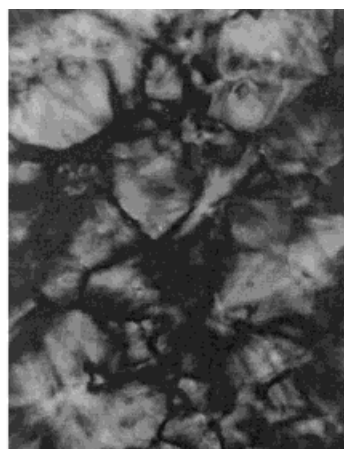
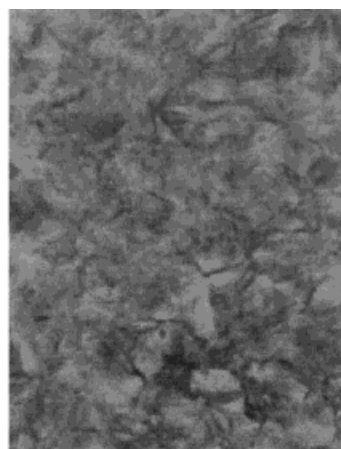


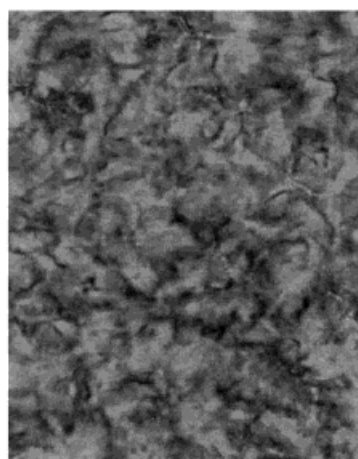
Figure 6 Dimension change vs. temperature curves for the UV-irradiated iPP.



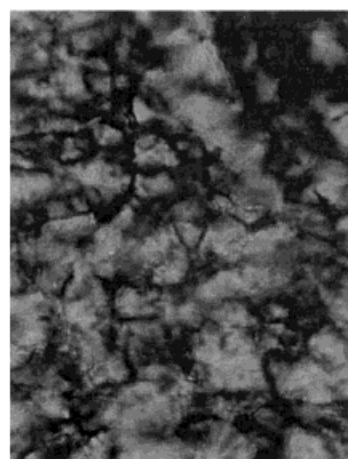
a. UV irradiation time, 0 hr



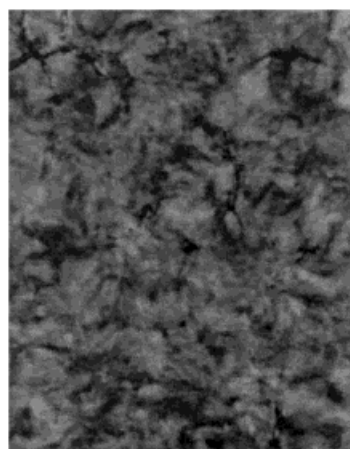
b. UV irradiation time, 0.5hr



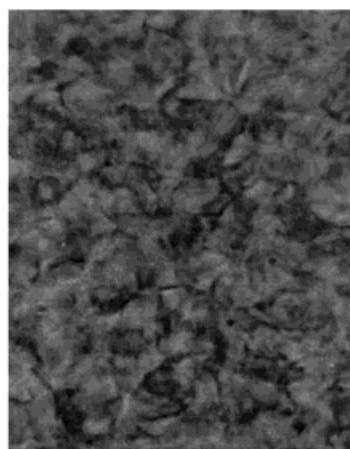
c. UV irradiation time, 1.0 hr



d. UV irradiation time, 1.5 hr



e. UV irradiation time, 2.0 hr



f. UV irradiation time, 2.5 hr

Figure 7 Polariscope photograph of the UV-irradiated PP (isothermal crystallization at 130°C for 1 h, $\times 640$).

Mechanical Measurement

Tables VIII and IX present the mechanical measurement results of the iPP samples. It is evident that the tensile and impact strength, the elongation at break, and the Young's modulus of the UV iPP are larger than that of the non-UV iPP. This type of behavior is related to the transition of α -phase to β -phase and the increasing crystallinity caused by the UV irradiation. Higher β -phase content is good for enhancing the toughness and strength. Considering DSC analysis, it can be seen that the relative level of β -phase is reduced in the 2.5 h UV time condition, the same as the tensile strength, Young's modulus, and elongation at break of the UV 2.5 h iPP sample.

In comparison the UV 1.5 h iPP with the non-UV iPP, the tensile and impact strength, the elongation at break, and the Young's modulus are increased to 35.3 MPa, 608.5 J/m, 579% and 1328 MPa, from 33.1 MPa, 528.6 J/m, 327% and 1183 MPa, respectively. Pabiot²⁹ revealed that the ultimate mechanical characteristics (especially elongation at break) of polyolefines are more sensitive to irradiation than methods reflecting chemical changes, so the elongation at break can be used to express the toughness of iPP. From this point of view, it can be seen that after the UV irradiation, the toughness of iPP has been improved within 2.5 h UV time.

CONCLUSIONS

In summary, the lower energy ultraviolet irradiation in less than a few hours is able to change the crystalline structures of iPP. The changes in crystalline structure lead to the crystalline phase transition of the α -phase to β -phase, and this is beneficial to increase the toughness of iPP. The content of

Table VIII Mechanical Properties of the Ultraviolet-Irradiated PP

UV Irradiation Time (h)	σ (MPa)	E (MPa)	ε_b (%)	Flexural Modulus (MPa)
0	33.1	1183	327	1411
0.5	36.1	1319	457	1318
1.0	34.4	1292	570	1279
1.5	35.3	1328	579	1244
2.0	34.7	1307	378	1230
2.5	34.6	1295	377	1200

Table IX Impact Strength of UV-Irradiated iPP

UV Irradiation Time (h)	Impact Strength (J/m)	Notched Impact Strength (J/m)
0	528.6	32.9
0.5	572.1	32.0
1.0	573.1	35.1
1.5	608.5	45.0
2.0	509.4	33.0
2.5	764.8	30.6

β -phase and the crystallinity of the UV iPP can be controlled via the UV irradiation time. The β -phase crystallize preferably within 2 h UV time, whereas the crystallinity is increased with increasing UV time, as demonstrated by DSC and WAXD measurements. The TG and TMA analysis show that for the UV iPP, the thermal degradation temperature and the thermal stability are largely raised, and the thermomechanical deformation decreases. Polariscopes observation reveals that the crystalline morphology of the UV iPP has been changed. After a short time UV irradiation, the mechanical properties of iPP are enhanced, especially toughness. In comparison with the non-UV iPP, the tensile and impact strength, the elongation at break, and the Young's modulus of the UV 1.5 h iPP are increased to 35.3 MPa, 608.5 J/m, 579% and 1328 MPa from 33.1 MPa, 528.6 J/m, 327% and 1183 MPa, respectively. In one word, functionalization of iPP by lower ultraviolet irradiation is able to improve the iPP properties under the considered experimental conditions.

REFERENCES

- De Roover, B.; Sclavons, M.; Carlier, V.; Devaaux, J.; Legras, R.; Momtaz, A. *J Appl Polym Sci* 1995, 33, 829.
- Xu, X. Proceeding of the Third China-Japan Seminar on Advanced Engineering Plastics, Polymer Alloys and Composites, 1 (1998).
- Tidjani, A.; Watanabe, Y. *J Appl Polym Sci* 1996, 60, 1839.
- Thorat, H. B.; Prabhu, C. S.; Kumar, S.; Pandya, M. V. *J Appl Polym Sci* 1996, 59, 1769.
- Van Gisbergen, J. G. M.; Meijer, H. E. H.; Lemstra, D. J. *Polymer* 1989, 30, 2153.
- Karpukhin, O. N.; Slobodetskaya, E. M. *J Polym Sci A1* 1979, 17, 3687.

7. Rabek, J. F. *Polymer Photodegradation*; Chapman & Hall: London, 1995; p 69, p 508.
8. Katan, E.; Narkis, M.; Siegmann, A. *J Appl Polym Sci* 1998, 70, 147.
9. Raab, M.; Kotulak, L.; Kolarik, J.; Pospisl, J. *J Appl Polym Sci* 1982, 27, 2457.
10. Akay, G.; Tincer, T.; Aydin, E. *Eur Polym J* 1980, 16, 599.
11. Allen, N. S.; Fatinikum, K. O.; Gardette, J. L.; Lemaire, J. *Polym Degrad Stabil* 1982, 4, 95.
12. Carlsson, D. J.; Garton, A.; Wiles, D. M. *Macromolecules* 1976, 9, 695.
13. Faucitano, A.; Buttafava, A.; Cominciolo, V. *Polym Photochem* 1986, 7, 491.
14. George, G. A.; Ghaemy, M. *Polym Degrad Stabil* 1991, 33, 411.
15. Schollenberg, C. S.; Meijer, H. D. F. *Polymer* 1991, 32, 438.
16. Tidjani, A. *J Appl Polym Sci* 1997, 64, 2497.
17. Shukla, S. R.; Athalye, A. R. *J Appl Polym Sci* 1994, 51, 1567.
18. Nito, K.; Suzuki, S. I.; Miyasaka, K.; Ishikawa, K. *J Appl Polym Sci* 1982, 27, 637.
19. Zhang, P. Y.; Ranby, B. *J Appl Polym Sci* 1990, 41, 1469.
20. Pasternak, M. *J Appl Polym Sci* 1995, 57, 1211.
21. Uzomah, T. C.; Unuoha, G. C. *J Appl Polym Sci* 1998, 69, 2533.
22. Carlsson, D. J.; Wiles, D. M. *Macromolecules* 1969, 2, 587.
23. Lacoste, J.; Carlsson, D. J. *J Polym Sci A1* 1992, 30, 493.
24. Aboulfaraj, M.; Ulrich, B.; Dahoun, A.; G'Shell, C. *Polymer* 1983, 24, 693.
25. Rabello, M. S.; White, J. R. *J Appl Polym Sci* 1997, 64, 2505.
26. Huang, M. R.; Li, X. G.; Fang, B. R. *J Appl Polym Sci* 1995, 56, 1323.
27. Karger-Kocsis, J.; Varga, J. *J Appl Polym Sci* 1996, 62, 29.
28. Turner Jones, A. *Polymer* 1971, 12, 487.
29. Pabiot, J.; Verdu, J. *Polym Eng Sci* 1981, 21, 32.